Conf-901125--2

CONF-901125--2

DE91 000392

STRESS-DISPLACEMENT RELATION DURING FIBER PULLOUT

C. H. Hsueh, Metals and Ceramics Division, Oak Ridge National Laboratory, Oak Ridge, TN 37831

ABSTRACT

During fiber pullout tests of fiber-reinforced composites, initial debonding, partial debonding, complete debonding at the interface, and fiber pullout occur sequentially. Adopting the shear lag model for stress analyses and the strength criterion for interfacial debonding, a bond length dependence of the initial debond stress is derived. During partial debonding, the stress initially increases with the increasing fiber displacement. The partial debond stress reaches a maximum value and begins to decrease with an accompanying decreasing fiber displacement until the interface is completely debonded. Theoretically, the stress-displacement curve shows a "nose" at the maximum debond stress. However, the pullout test is generally conducted under the condition of an increasing fiber displacement. Hence, at the maximum debond stress, the observed stress drops abruptly as the increasing fiber displacement type test obscures the nose-type characteristic.

1. INTRODUCTION

The fiber pullout test has been used to study the interfacial properties of fiber-reinforced ceramic composites [1-3]. Based on the shear lag model, axial loading of the fiber results in a maximum interfacial shear stress at the surface which depends on the bonded fiber length [1-3]. Adopting the strength criterion for debonding at the fiber-matrix interface, interfacial debonding occurs when the interfacial shear stress overcomes the interfacial shear strength. Hence, interfacial debonding initiates at the surface during fiber pullout. Residual clamping stresses often exist at the interface and result in interfacial friction for the debonded interface. After initial debonding, further debonding requires the applied stress to overcome both the interfacial frictional stress of the debonded interface and the bond strength at the end of the debonded interface. After complete debonding, fiber pullout requires the applied stress to overcome the

"The submitted manuscript has been authored by a contractor of the U.S. Government under contract No. DE-AC05-84OR21400. Accordingly, the U.S. Government retains a nonexclusive, royalty-free license to publish or reproduce the published form of this contribution, or allow others to do so, for U.S. Government purposes.

interfacial frictional stress along the entire fiber length. The purpose of the present study is to examine the stress-displacement relation during such fiber pullout.

2. ANALYSES

The shear lag model is shown in Fig. 1. A fiber with a radius, a, is located at the center of a coaxial cylindrical shell of matrix with an outer radius, b, where z is the direction parallel to the fiber axis, t is the thickness of the composite, and h is the debond length. The fiber is subjected to a residual clamping stress, σ_c, at the interface. An axial stress, σ_o, is applied on the fiber at the surface, $z=t$, and the stress transfers from the fiber to the matrix through the interfacial shear stress.

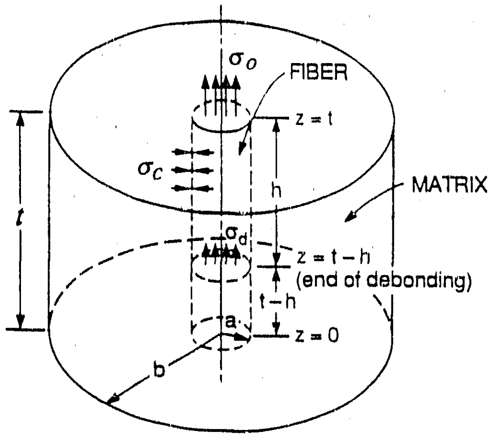

Fig. 1. A schematic diagram showing the shear lag model and partial debonding during fiber pullout.

At the end of debonding length ($z=t-h$), the interfacial shear stress reaches the interfacial shear strength, τ_s, and the corresponding axial stress in the fiber reaches the interfacial bond strength, σ_d, which has been derived such that [4,5]:

$$\sigma_d = \frac{-2\tau_s\left\{(1+\nu_m)\left[1+\left(\frac{b^2}{a^2}-1\right)\frac{E_m}{E_f}\right]\left[b^2\ln\left(\frac{b}{a}\right)-\frac{b^2-a^2}{2}\right]\right\}^{1/2}}{a\left(\frac{b^2}{a^2}-1\right)\left(\frac{E_m}{E_f}\right)\coth[\alpha(t-h)]+\frac{2}{\exp[\alpha(t-h)]-\exp[-\alpha(t-h)]}} \tag{1}$$

where t-h is the bonded fiber length (see Fig. 1), E and ν are Young's modulus and Poisson's ratio, the subscripts f and m denote the fiber and the matrix, respectively, and α is given by:

$$\alpha = \frac{1}{a}\left\{\frac{a^2 E_f + \left(b^2 - a^2\right)E_m}{E_f\left(1+\nu_m\right)\left[b^2 \ln\left(\frac{b}{a}\right) - \frac{b^2 - a^2}{2}\right]}\right\}^{1/2} \quad (2)$$

When $h=0$ in Eq. (1), σ_d becomes the stress required for initial debonding. The axial displacement of the fiber at the surface of the composite, u, has been analyzed for the fiber pullout process, where the interface is initially bonded, partially debonded, completely debonded and finally the fiber is pulled out [5].

When the applied axial stress is lower than σ_d, the interface remains bonded. The relation between the fiber displacement, u_b, the applied stress, σ_o, and the bond length, t, is [5] :

$$u_b = \frac{a^2\sigma_o}{a^2 E_f + \left(b^2 - a^2\right)E_m}\left\{t + \frac{1}{\alpha}\left[\left(\frac{b^2}{a^2} - 1\right)\frac{E_m}{E_f} - 1\right]\left[\frac{\exp(\alpha t) + \exp(-\alpha t) - 2}{\exp(\alpha t) - \exp(-\alpha t)}\right]\right\} \quad (3)$$

A linear relation between u_b and σ_o is obtained for a bonded interface. The fiber displacement, u_b, given by Eq. (3) consists of two components ($u=u_b=u_o+u_r$, see Fig. 2a) : 1) the overall displacement of the composite, u_o, given by:

$$u_o = \frac{a^2 t\sigma_o}{a^2 E_f + \left(b^2 - a^2\right)E_m} \quad (4)$$

which is linearly proportional to the bond length, t, and 2) the average relative displacement between the fiber and the composite, u_r, given by:

$$u_r = \frac{a^2\sigma_o}{a^2 E_f + \left(b^2 - a^2\right)E_m}\frac{1}{\alpha}\left[\left(\frac{b^2}{a^2} - 1\right)\left(\frac{E_m}{E_f}\right) - 1\right]\left[\frac{\exp(\alpha t) + \exp(-\alpha t) - 2}{\exp(\alpha t) - \exp(-\alpha t)}\right] \quad (5)$$

which approaches an asymptotic value when t approaches infinity.

During partial debonding, the total displacement, u, consists of two components ($u=u_b+u_s$, see Fig. 2b) : 1) the displacement, u_b, for the portion of the fiber remaining bonded to the matrix (with bond length t-h), and 2) the displacement due to relative sliding between the fiber and the matrix, u_s, for the debond length, h, which was given in Ref. [5]. At complete debonding, the fiber displacement results only from the relative sliding between the fiber and the matrix along the entire fiber length (i.e., $u=u_s$).

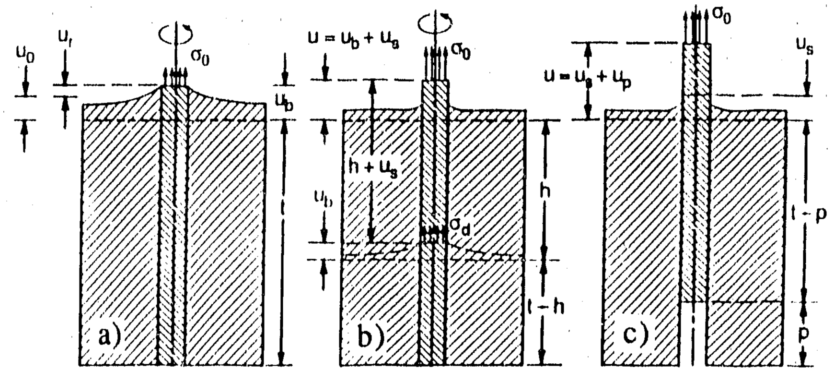

Fig. 2. Schematic diagram showing the fiber displacement during the fiber pullout test for a) a bonded interface, ($\sigma_o<\sigma_d$), b) partial debonding ($\sigma_o>\sigma_d$), and c) fiber pullout: ----- indicating position before loading.

During fiber pullout, the total fiber displacement also consists of two components ($u=u_s+u_p$, see Fig. 2c) : 1) the displacement due to relative sliding, u_s, for the portion of the fiber remaining in the matrix, and 2) the displacement due to the portion of the fiber being pulled out, u_p.

3. RESULTS

The specific results are computed using properties of materials of a single stainless steel-fiber-reinforced epoxy resin matrix [2] where E_f= 170 GPa, E_m=3.65 GPa, v_f=0.35, v_m=0.39, a=75 μm and b=7.5 mm. The residual radial stress, σ_c, is -12.25 MPa, and the interfacial shear strength, τ_s, is -37 MPa. The calculated ratio of the bond strength to the interfacial shear strength, σ_d/τ_s, as a function of the normalized bond length, $(t-h)/a$, is shown in Fig. 3. The bond strength increases from zero and reaches an asymptotic value as the bond length increases from zero to some finite value.

The relation between the applied stress, σ_o, and the debond length, h, during partial debonding is shown in Fig. 4 for different thicknesses of the composite, t. At a fixed thickness, the bond length decreases with increasing debond length. Hence, from initial debonding to complete debonding, while the stress required to overcome the interfacial friction increases, σ_d is initially constant and then decreases to zero (see Fig. 3). Figure 4 shows that depending on the balance between these two stress components, σ_o increases to a maximum value and then decreases during partial debonding. At the end of the curve, complete debonding and fiber pullout occur.

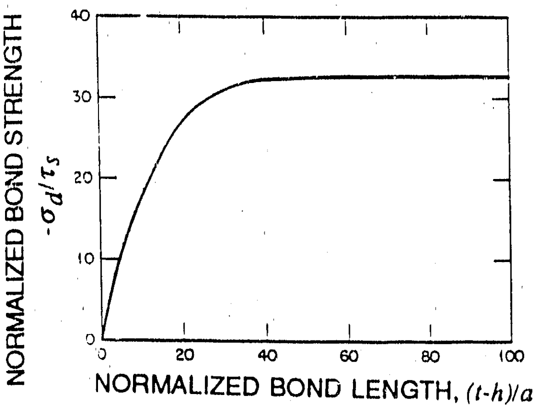

Fig. 3. The calculated ratio of the bond strength to the interfacial shear strength, $-\sigma_d/\tau_s$, as a function of the normalized bond length, $(t-h)/a$, for steel fiber-epoxy resin composite.

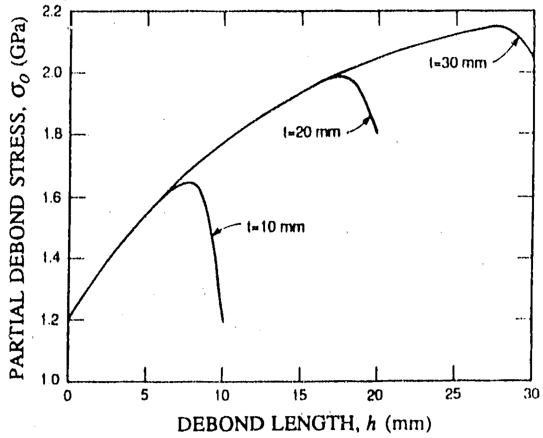

Fig. 4. The calculated partial debond stress, σ_o, as a function of the debond length, h, at different thicknesses, t, for steel fiber-epoxy resin composites.

The applied stress versus fiber displacement relation is shown in Fig. 5 at different thicknesses emphasizing two regimes of the fiber displacement. When u is small, the detailed portion of the curve during debonding is shown in Fig. 5a. During fiber pullout, u is relatively larger than that in Fig. 5a and is shown in Fig. 5b. When the applied stress is lower than the initial debond stress, the relation is linear. After initial debonding, σ_o increases nonlinearly with increasing u initially. The partial debond stress then reaches a maximum value and begins to decrease with an accompanying decreasing fiber displacement until the fiber is completely debonded. After complete debonding, fiber pullout occurs and the stress decreases with increasing u, where the negative curvature of the curve (see Fig. 5b) is due to Poisson's effect.

4. DISCUSSIONS

Fiber pullout with interfacial friction is a complicated problem. To obtain analytical solutions, certain simplifications are required. The essence of present analytical solutions is to satisfy as many boundary conditions as possible, and to approach the rest of boundary conditions as closely as possible. The approximations used in the present study are [4-7]: 1) For a fiber with small radius in the composite (i.e., $a<<b$), the axial stress in the fiber is assumed to be independent of the radial coordinate, r. 2) To approximate the radial dependence of the axial stress in the matrix, the shear stress in the matrix is assumed to be inversely proportional to r. 3) To relate the tangential stress to the radial stress at the interface, a plane strain condition is assumed.

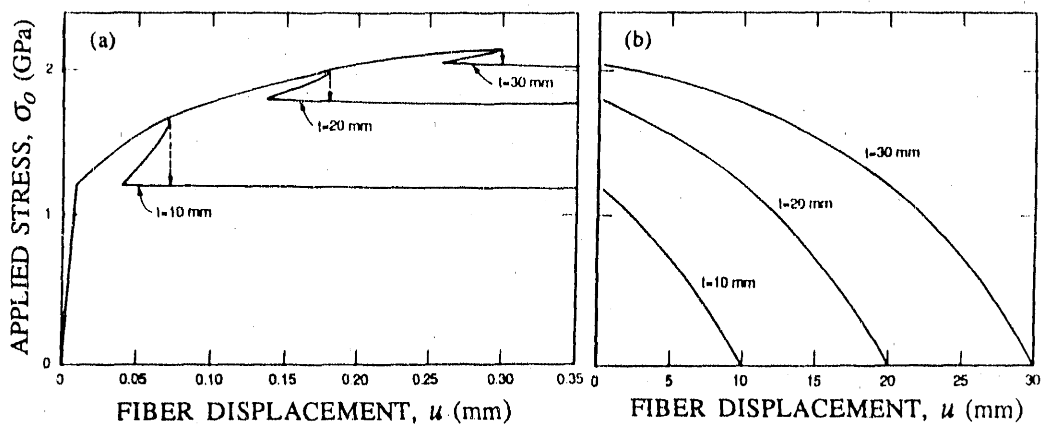

Fig. 5. The applied stress, σ_o, as a function of the axial displacement of the fiber, u, at different thicknesses, t, for steel fiber-epoxy resin composites for: a) elastic loading, partial debonding and complete debonding (-----, load drop to keep u increasing in the experiment), and b) fiber pullout.

The residual stress considered in the present study is in the radial direction only. In the presence of the residual axial stress, an interfacial shear stress is induced by the residual axial stress when the interface is bonded [6]. In this case, the applied axial stress on the fiber required to debond the interface is modified by the presence of the residual axial stress. When the interfacial shear stresses induced by the residual axial stress and by the applied axial stress are in the same direction, the existence of the residual axial stress facilitates debonding. Conversely, interfacial debonding is inhibited. For a partially debonded interface, the residual axial stress influences the boundary condition at the end of debonding which, in turn, modifies the stress distribution in the debonded region. For a completely debonded interface, the stress required to pull the fiber out is independent of the residual axial stress, which is relaxed due to complete debonding.

For an unbonded or a weak interface, sliding at the fiber-matrix interface can occur due to residual stresses, which result from mismatch strains between the fiber and the matrix. The sliding length and the stress distribution in the composite have been analyzed [7]. The results show that the sliding length is limited by the interfacial friction. The fiber can pop out or sink beneath the surface of the composite depending mainly on the mismatch strain in the axial direction. However, the sliding phenomena are modified by the mismatch strain in the radial direction. For example, when the interface is subjected to residual radial compression, in the absence of the axial mismatch strain, the fiber can pop out of the surface because of Poisson's effect.

ACKNOWLEDGEMENT

The author thanks Drs. P. F. Becher, A. Bleier and H. T, Lin for reviewing the manuscript. Research sponsored by Division of Materials Sciences, Office of Basic Energy Sciences, U.S. Department of Energy, under contract DE-AC05-84OR21400 with Martin Marietta Energy Systems, Inc.

REFERENCES

1. P. Lawrence, "Some Theoretical Considerations of Fiber Pullout from an Elastic Matrix," J. Mater. Sci., 1 [1] (1972) 1-6.
2. A. Takaku and R. G. C. Arridge, "The Effect of Interfacial Radial and Shear Stress on Fiber Pull-out in Composite Materials," J. Phys. D: Appl. Phys., 6 (1973) 2038-2047.
3. J. K. Wells and P. W. R. Beaumont, "Debonding and Pull-out Processes in Fibrous Composites," J. Mater. Sci., 20 [4] (1985) 1275-1284.
4. C. H. Hsueh, "Interfacial Debonding and Fiber Pull-out Stresses for Fiber-Reinforced Composites," Mater. Sci. Eng., A123 [1] (1990) 1-11.
5. C. H. Hsueh, "Interfacial Debonding and Fiber Pull-out Stresses for Fiber-Reinforced Composites, II: Non-constant Interfacial Bond Strength," Mater. Sci. Eng., A125 [5] (1990) 67-73.
6. C. H. Hsueh, "Interfacial Debonding and Fiber Pull-out Stresses for Fiber-Reinforced Composites, III: with Residual Radial and Axial Stresses," submitted to Mater. Sci. Eng.
7. C. H. Hsueh, "Interfacial Debonding and Fiber Pull-out Stresses for Fiber-Reinforced Composites, IV: Sliding due to Residual Stresses," to be submitted to Mater. Sci. Eng.

-END-

DATE FILMED

11 / 05 / 90